Diffusion of hydrogen interstitials in the near-surface region of Pd(111) under the influence of surface coverage and external static electric fields

M. Blanco-Rey and J. C. Tremblay

Citation: The Journal of Chemical Physics **142**, 154704 (2015); doi: 10.1063/1.4917537

View online: http://dx.doi.org/10.1063/1.4917537

View Table of Contents: http://scitation.aip.org/content/aip/journal/jcp/142/15?ver=pdfcov

Published by the AIP Publishing

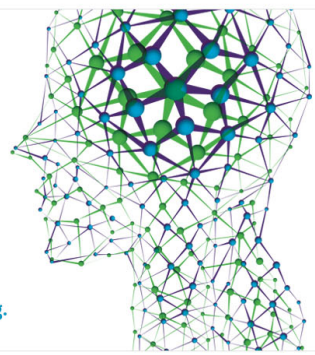

Diffusion of hydrogen interstitials in the near-surface region of Pd(111) under the influence of surface coverage and external static electric fields

M. Blanco-Rey[1,2] and J. C. Tremblay[3]
[1]*Departamento de Física de Materiales, Facultad de Químicas UPV/EHU, Apartado 1072, 20018 Donostia-San Sebastián, Spain*
[2]*Donostia International Physics Center (DIPC), Paseo Manuel de Lardizabal 4, 20018 Donostia-San Sebastián, Spain*
[3]*Institute for Chemistry and Biochemistry, Freie Universität Berlin, Takustrasse 3, D-14195 Berlin, Germany*

(Received 30 January 2015; accepted 2 April 2015; published online 17 April 2015)

Past scanning tunneling microscopy (STM) experiments of H manipulation on Pd(111), at low temperature, have shown that it is possible to induce diffusion of surface species as well as of those deeply buried under the surface. Several questions remain open regarding the role of subsurface site occupancies. In the present work, the interaction potential of H atoms with Pd(111) under various H coverage conditions is determined by means of density functional theory calculations in order to provide an answer to two of these questions: (i) whether subsurface sites are the final locations for the H impurities that attempt to emerge from bulk regions, and (ii) whether penetration of the surface is a competing route of on-surface diffusion during depletion of surface H on densely covered Pd(111). We find that a high H coverage has the effect of blocking resurfacing of H atoms travelling from below, which would otherwise reach the surface *fcc* sites, but it hardly alters deeper diffusion energy barriers. Penetration is unlikely and restricted to high occupancies of *hcp* hollows. In agreement with experiments, the Pd lattice expands vertically as a consequence of H atoms being blocked at subsurface sites, and surface H enhances this expansion. STM tip effects are included in the calculations self-consistently as an external static electric field. The main contribution to the induced surface electric dipoles originates from the Pd substrate polarisability. We find that the electric field has a non-negligible effect on the H-Pd potential in the vicinity of the topmost Pd atomic layer, yet typical STM intensities of 1-2 $V Å^{-1}$ are insufficient to invert the stabilities of the surface and subsurface equilibrium sites. © *2015 AIP Publishing LLC.* [http://dx.doi.org/10.1063/1.4917537]

I. INTRODUCTION

Scanning tunneling microscopy (STM) has become a prominent tool for manipulation at the atomic scale in the surface science community. It was recently revealed that the use of STM as a manipulation tool is not restricted to the surface region in experiments where diffusion of diluted H[1] and D[2] beneath Pd(111) surfaces was accomplished. In the same context, too, it has been shown that upon application of STM voltage pulses on densely H-covered Pd(111) it is possible to achieve a reversible depletion of the adsorbed H atoms, where subsurface H atoms are thought to play an active role in the displacement of the adsorbates.[1,3] It is known that the catalytic properties of Pd extended surfaces and nanoparticles during (de)hydrogenation reactions are modified by the presence of H in the surface and subsurface.[4–8] Although the aforementioned experiments provide valuable recipes for producing nanopatterned H-rich regions at Pd(111), a precise characterisation of the final H-distributions is still missing. This is in part due to the fact that these H-distributions are the result of at least three major interacting factors: the inelastic scattering of tunnelling electron with the initial arrangement of H-impurities, thermal diffusion, and electrostatic effects induced by the closely lying STM tip. From this perspective, the outcome of the experiments cannot be easily anticipated. As a matter of fact, the provided interpretations of the modified Pd(111) STM images in Refs. 1 and 3 and the results of related theoretical works are in apparent contradiction.

To lift this ambiguity, the present paper deals with two ingredients that were either absent or incompletely investigated in earlier models of these experiments: the presence of preadsorbed H at the surface and the electric field exerted by the STM tip, which are examined here by means of *ab-initio* calculations within the density functional theory (DFT). In particular, we study in detail the potential energy landscape along fully relaxed one-dimensional reaction paths in order to answer the following questions: (i) Do H-impurities departing from the bulk region stop at subsurface sites upon STM manipulation of a Pd(111) surface in the absence of surface H species? (ii) When manipulation is carried out at highly H-covered Pd(111), does depletion happen as a consequence of penetration toward subsurface sites or is it due to on-surface diffusion?

The central experiment we aim at understanding is that of Sykes *et al.*,[1] which is carried out at $T = 4$ K in a highly dilute regime, with little or no surface H. In this case, the H-impurities are believed to be removed from buried layer interstices, where the tip field is almost completely screened out by the metal electrons. This means that H motion is mostly promoted by non-adiabatic coupling (NAC) with tunnelling

electrons. After application of tunneling currents, bright stripes are observed in the STM images, with variable brightness and thickness depending on the applied intensity and bias voltage. In topographic mode STM, these features appear to be as high as 0.1–0.6 Å with respect to the surrounding unmodified Pd(111). The stripes are interpreted as being formed by H displaced from the bulk to subsurface cavities, while the surface remains apparently clean. This interpretation is made on the basis that Pd atomic planes are known to undergo a net elevation when H is adsorbed at subsurface sites, albeit previous theoretical and experimental values in the literature are one order of magnitude smaller than those assigned by the protrusion brightness.[9,10] In addition, DFT calculations on the energetics of the system in the diluted regime show that the subsurface site is less stable than the *fcc* and *hcp* hollow sites on the surface (by values ranging in about 0.10-0.30 eV for coverages $\Theta = 1/3, 1/4$[10–14]), and also that the energy barrier for resurfacing at low coverages is rather low, of about 0.1 eV.[10,13–15] Based on these thermodynamical considerations, it appears that H atoms should lie on the surface after manipulation, unlike proposed in Ref. 1. Inelastic effects do neither support the H population of subsurface sites in the diluted regime: dynamical NAC modelling beyond the harmonic approximation has predicted that H atoms departing from buried sites will preferentially populate the Pd(111) surface hollows at long interaction times under simulation conditions comparable to the experimental ones.[16] In other words, the system has a quasi-thermal behaviour at long times and the final distribution of H is governed by the potential energy surface (PES) topography. One objective of the present study is to determine whether the observed protrusions contain H on the surface, too. This seems plausible, considering that some adsorbed species have a blocking effect for the resurfacing of interstitials. This is, for example, the case of CO adsorbed on Pd(111), which suppresses H resurfacing due to the strongly repulsive H-CO interaction.[17] Here, we might thus foresee that the first batch of H atoms displaced from the bulk resurfaces to form a dense (1×1) coverage, resulting in a blocking scenario where H accumulates at interstitials in the few outer Pd layers. This mechanism would answer our first question.

In another important study by Mitsui *et al.*[3] conducted on Pd(111) at higher temperatures (T = 40–90 K), STM experiments at high H-coverage ((1×1) overlayer) were performed (exposure at $T > 50$ K is necessary to form the (1×1) overlayer[18]). Application of an STM current induces surface H movement, resulting in triangle-shaped regions of nm^2 in size partially depleted from H. In these experiments, thermal and tip field effects, with estimated typical values of 1–2 V $Å^{-1}$, come into play. DFT calculations show that the field destabilises H, but it also seems that intense enough fields contribute to stabilising subsurface H. Therefore, the electrostatic effect is mostly responsible for the surface H depleted triangles on the one hand. On the other hand, under the experimental temperatures, thermal H diffusion is seen to dissolve the triangles at longer timescales. The presence of coadsorbed H hinders diffusion of surface species, which happens across the bridge between the *fcc* and *hcp* hollows. Experimentally, at coverages $\Theta > 2/3$, a diffusion activation barrier of 0.21 eV is found at $T = 37$ K, whereas for isolated H adsorbates it is 0.09 eV, found at $T = 65$ K.[18] In experiments at $T = 4$ K, the onset of surface diffusion at low coverage is observed at a bias voltage of 0.07-0.10 eV, but generalised motion of surface atoms requires at least 0.15 V.[19] These values are consistent with DFT barriers of 0.12-0.15 eV.[3,10,20] Calculated barriers for low coverage surface penetration are 0.40–0.46 eV.[3,12,14,21] Although these are larger barriers than for resurfacing and on-surface diffusion, precoverage effects, an intense field, or the combination of both could eventually favour penetration over the other mechanisms. Also, the effect of preadsorbed H is not fully understood yet. It has been studied by DFT at (1×1) periodic supercells, where penetration barriers ranging from 0.33 eV[11] to 0.74-0.76 eV[12] have been reported depending on the surface model used. The extent of the changes these effects induce in the H-Pd surface interaction potential will help us answer the second question posed above. As already mentioned, in the clean surface it was found that the system behaves quasi-thermally under STM current injection, but significant changes in the PES brought by coverage and field effects might alter this picture. As a matter of fact, the DFT investigations presented here serve as a basis for a quantum dynamical study to be published elsewhere.[22]

The paper is organised as follows: Sec. II deals with the calculations details. The results are split into two Subsections III A and III B, that describe the effect of H-adsorbates and electric fields, respectively, on the system energetics and surface dipoles. The results are discussed in Sec. IV and finally conclusions are drawn.

II. METHODOLOGY

We calculate self-consistently by DFT the potential energies for a H atom penetrating a clean and several H-covered Pd(111) slabs. Since we use slabs of finite thickness in periodic supercells to represent the surface, the DFT calculations are carried out with plane wave basis sets, as implemented in the Quantum Espresso package.[23] We describe the ion cores with scalar relativistic ultrasoft pseudopotentials[24] and we treat the exchange and correlation functional in the PBE formulation of the generalised gradient approximation.[25] The Pd(111) surface is modelled by a slab consisting of six Pd layers separated by a vacuum region equivalent to five times the interlayer separation (11.43 Å) and (2×2) lateral periodicity, where the in-plane Pd-Pd distance is $a_0 = 2.80$ Å. In the plane wave expansion, the cut-off energies are 25 Ry and 250 Ry for the wavefunctions and charge density, respectively, and we use a $8 \times 8 \times 1$ Monkhorst-Pack special k-point mesh.[26] The convergence energy threshold for the self-consistent determination of the wavefunctions is 10^{-7} Ry. In the structural relaxations, all the atoms except for the bottom Pd layer are allowed to move, and the forces on the atoms are converged with a tolerance of 2×10^{-4} Ry $Å^{-1}$.

When H atoms are adsorbed on the slab, a dipole appears on the surface. Its magnitude is calculated following the procedure described in Refs. 27 and 28, which consists in placing a dummy charged thin slab in the vacuum region between the Pd slabs that compensates the linear term in the crystal potential produced by the surface dipoles. The perpendicular dipole per unit cell, μ_0, results in a jump in

the potential across the charged slab of

$$\Delta V = -8\pi\mu_0/A, \tag{1}$$

where A is the unit cell area. This magnitude is thus equivalent to the adsorbate induced change in the surface work function, $\Delta\Phi$. The same methodology allows to converge wavefunctions self-consistently under an external electric field, $\mathbf{E}_{ext}$. In this work, we have considered fields perpendicular to the surface with magnitudes of the order of 0.02 a.u. ($\simeq$1 V Å^{-1}), which is a representative value of the characteristic electric fields exerted by an STM tip on the surface.

Upon application of the perpendicular electric field, the charge density in the slab is redistributed to ensure that the field inside the metal is zero. For $E_{ext} > 0$, charge depletion occurs at the top of the slab and charge is accumulated at the bottom, and vice versa for $E_{ext} < 0$. Therefore, a net dipole appears that is slab thickness dependent. This dependence is avoided and the dipole value of the top face of the slab (where adsorbates are placed) is isolated as follows. First, we define a plane averaged charge density:

$$\rho_{av}(z; E_{ext}) = \int\int_{s.u.c.} \rho(x, y, z; E_{ext})\mathrm{d}x\mathrm{d}y, \tag{2}$$

where the integral of the charge density, ρ, is performed in the (2×2) surface unit cell (s.u.c.). The charge density difference (CDD) between the field-switched-on and field-switched-off states, is given by

$$\Delta\rho_{av}(z; E_{ext}) = \rho_{av}(z; E_{ext}) - \rho_{av}(z; 0). \tag{3}$$

This quantity is then used to calculate the induced dipole at the surface by a field E_{ext}[29]:

$$\mu_{ind}(E_{ext}) = \int_{z_1}^{z_2} z\Delta\rho_{av}(z; E_{ext})\mathrm{d}z \tag{4}$$

where the integration interval $[z_1, z_2]$ goes from the centre of the metal slab, where the electric field is assumed to be completely screened out, to the centre of the vacuum region between periodic slabs.

III. RESULTS

A. Coverage dependence of geometries, potential energies, and surface dipoles

We have investigated four different surfaces as hosts for a H atom impurity: a clean Pd(111), two surfaces with coverage $\Theta = 1$, where H saturates *fcc* and *hcp* hollow sites, and a fourth one with coverage $\Theta = 0.75$, where H adsorbates lie at *fcc* sites. The equilibrium heights of the H adsorbates in these configurations are shown in Table I. A spontaneous electric dipole, μ_0, appears at the surface due to the coverage that alters the work function value calculated for clean Pd(111), $\Phi = 5.28$ eV (the experimental value is $\Phi = 5.6$ eV[30]). For H atoms on Pd(111), the surface dipole points inward, which is consistent with the adsorbates being electron acceptors, and thus it increases the value of Φ. These electrostatic properties are also summarised in Table I. The results found for the highest coverage are in good agreement with the experimental value $\Delta\Phi = 0.18$ eV.[31] Agreement is also good between the quantities shown in Table I and theoretical literature values.[10–12,14,20,32,33] The properties at intermediate coverages $\Theta = 1/9, 1/4$ are also shown (see Ref. 34).

TABLE I. Properties of bare slabs: vertical displacement of the top layer (Pd1) of the slab (Δz_{Pd1}), height of the H adsorbate above the Pd1 layer (h_H), spontaneous dipole in the unit cell (a (3×3) one for $\Theta = 1/9$ and a (2×2) one for the other cases) and increase in the work function $\Delta\Phi$, with the clean Pd(111) $\Phi = 5.28$ eV.

Θ-site	Δz_{Pd1}	h_H (Å)	μ_0 (D)	$\Delta\Phi$ (eV)
0	0.105	...	...	...
fcc − Θ = 1/9	0.064	0.811	−0.065	0.040
fcc − Θ = 1/4	0.126	0.816	−0.066	0.091
fcc − Θ = 3/4	0.159	0.816	−0.143	0.199
fcc − Θ = 1	0.173	0.824	−0.138	0.191
hcp − Θ = 1	0.189	0.827	−0.130	0.180

The H atom impurity resurfaces through an *fcc* site. In the $\Theta = 0.75$ case, the empty *fcc* site is used. In the *fcc* − Θ = 1 case, the impurity displaces the adsorbates toward the *hcp* sites as it passes by the topmost Pd layer, denoted Pd1 hereafter. Transfer of the H atom impurity at the Pd near-surface region happens through a similar pathway to that known for diffusion in the bulk, namely, that the H atom jumps alternately between octahedral and (less stable) tetrahedral sites. Therefore, a H atom penetrating or resurfacing in Pd(111) is reasonably well modelled by a staircase-shaped one-dimensional pathway, as sketched in Fig. 1, which features perpendicular segments and shorter lateral ones. The potential energies along the one-dimensional pathways shown in Fig. 2 are calculated keeping the z (x, y, z) coordinate(s) of the impurity constrained along the segments perpendicular (parallel) to the surface and relaxing the remaining degrees of freedom in the system. In this figure, the reaction coordinate, r, is the distance along the one-dimensional pathway, taking positive (negative) values outside (inside) the slab. We have verified using the nudge elastic band

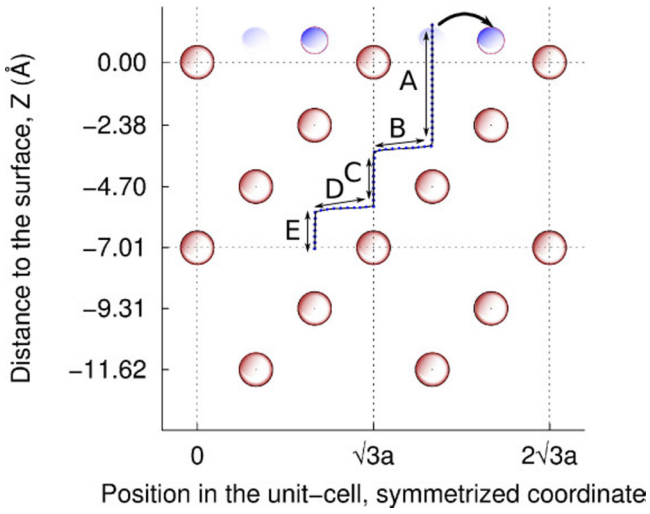

FIG. 1. Sketch of the staircase-shaped one-dimensional pathway for resurfacing of H atoms from bulk-like positions (b, at $z_H \sim 5.6$ Å) to the surface through the *fcc* hollow. In the case of a *fcc* − Θ = 1 covered surface, the curved arrow indicates that the H-adsorbate is displaced to the *hcp* site by the repulsive interaction with the emerging atom.

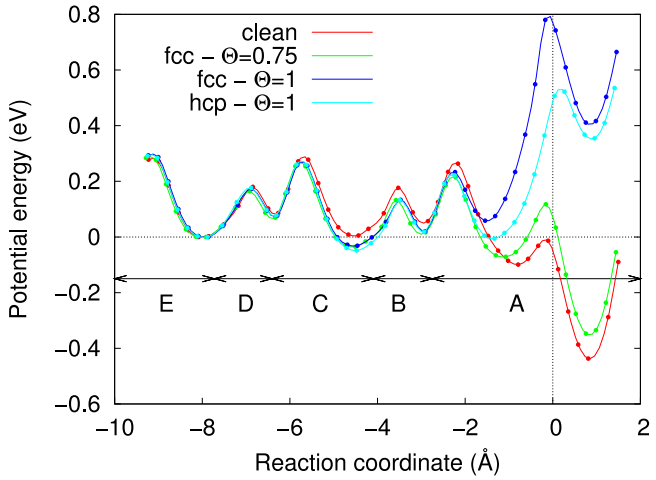

FIG. 2. One dimensional potential energy for H penetrating the host slabs at different coverages along the minimum energy pathway. The reaction coordinate and pathway segment labels are shown in Fig. 1 The dots are the DFT calculated values and lines are a spline interpolation to guide the eye. The common energy zero for all the slabs is chosen at the deepest octahedral site (O_b). The reaction coordinate origin is set where the H impurity height coincides with the equilibrium height of the topmost Pd layer in each host surface.

method[35,36] that the 90° turns in the pathway and the smaller barriers in the potential found, in the constrained calculations, are realistic. We will discuss the results in terms of the four main minima corresponding to octahedral environments, which are denoted as surface (S) at $r \simeq 1$ Å ($z_H \simeq 1.0$ Å), subsurface (O_{ss}) at $r \simeq -1$ Å ($z_H \simeq -0.8$ Å), sub-subsurface (O_{sb}) at $r \simeq -4.2$ Å ($z_H \simeq -3.3$ Å), and bulk sites (O_b) $r \simeq -8$ Å ($z_H \simeq -5.6$ Å). We observe that the influence of the surface coverage is of only a few meV at the O_{sb} site, and that it becomes negligible at the O_b site. In the clean surface, we obtain a barrier for resurfacing $E_a(O_{ss} \rightarrow S) = 0.065$ eV, and 0.42 eV for the reverse processes (same as found in Ref. 21). These values, which are in agreement with those of Ref. 17, are lower than the ones reported for a three-dimensional potential in an unrelaxed Pd(111) lattice.[10,11,13] In all the studied cases, relaxation has the effect of lowering down the diffusion barriers by ~0.1 eV and of further stabilizing the S site. The diffusion barriers, E_a, and reaction energies, $E_r = E_{\text{reactant}} - E_{\text{product}}$, are summarised in Table II, including both transfers to adjacent octahedral cavities and intermediate tetrahedral ones. Finally, an activation barrier of $E_a = 0.138$ eV is found for diffusion on the clean surface from a *fcc* to a *hcp* hollow. This barrier is located at the bridge position. The *hcp* site is slightly less stable than the *fcc* one by 0.03 eV. A tetrahedral stable subsurface site exists below the *hcp*, as found in Ref. 20, which we label $T_{ss,hcp}$. The barrier for penetration to the latter site from the *hcp* hollow is 0.410 eV, and the reverse resurfacing process has a barrier of 0.067 eV. Following a nearly horizontal pathway below the surface, which has a 0.038 eV barrier, the H impurity may arrive at the O_{ss} site. Since these values are similar to $E_a(S \rightarrow O_{ss})$ and $E_a(O_{ss} \rightarrow S)$, respectively, we can expect similar likelihoods for penetration and resurfacing processes at the surface *fcc* and *hcp* hollows.

Fig. 3 shows the vertical displacements from their equilibrium average z coordinates of the five mobile Pd layers in each slab (Pd1 to Pd5) as a function of the z coordinate of the H impurity, z_H, as it travels through the near-surface region. The top Pd1 layer displacement is the magnitude that can be compared directly with the observed lattice expansions in the STM experiments. As a general trend, the outer Pd layers are upward (downward) shifted by a H impurity that lies immediately below (above) a Pd layer. As shown in Fig. 3, the upward shifts are larger in magnitude, specially at the outer layers in densely covered surfaces when the H impurity lies below the Pd1 layer. The Pd1 layer shift takes a maximum value of 0.40 Å for the $fcc - \Theta = 1$ surface, in contrast with the clean case, where it is only of 0.13 Å. Under this configuration, the Pd1 layer appears to be non-negligibly buckled in the $\Theta = 1$ cases (the heights of the highest and lowest Pd atoms within the Pd1 layer differ about 0.05 Å, and values are slightly larger when the H lies almost in-plane, as shown in Fig. 3). This location of the H atom affects not just the closest Pd layer position, but also deeper ones. For example, when the H impurity lies immediately below Pd2, but still a few tenths of Å above the O_{ss} site, in the $fcc - \Theta = 1$ (clean) slab, Pd2 is shifted 0.27 Å (0.12 Å). In the studied intermediate coverage, $fcc - \Theta = 0.75$, relaxations take values that are closer to those

TABLE II. Reaction energies and barriers in Fig. 2 in eV considering only the octahedral site values. In brackets, the two intermediate barriers for those processes that result from considering the tetrahedral sites, too.

	Clean	$fcc-\Theta=3/4$	$fcc-\Theta=1$	$hcp-\Theta=1$
$E(O_{sb})-E(O_b)$	0.006	−0.035	−0.031	−0.049
$E(O_{ss})-E(O_{sb})$	−0.084	−0.036	0.090	0.043
$E(S)-E(O_{ss})$	−0.358	−0.276	0.352	0.360
$E_a(O_b \rightarrow O_{sb})$	0.278	0.254	0.258	0.260
	(0.181)	(0.165)	(0.176)	(0.176)
	(0.192)	(0.184)	(0.182)	(0.182)
$E_a(O_{sb} \rightarrow O_b)$	0.272	0.289	0.289	0.309
$E_a(O_{sb} \rightarrow O_{ss})$	0.258	0.249	0.264	0.271
	(0.171)	(0.168)	(0.165)	(0.181)
	(0.207)	(0.198)	(0.213)	(0.203)
$E_a(O_{ss} \rightarrow O_{sb})$	0.342	0.285	0.175	0.227
$E_a(O_{ss} \rightarrow S)$	0.065	0.189	0.721	0.528
$E_a(S \rightarrow O_{ss})$	0.424	0.465	0.369	0.168

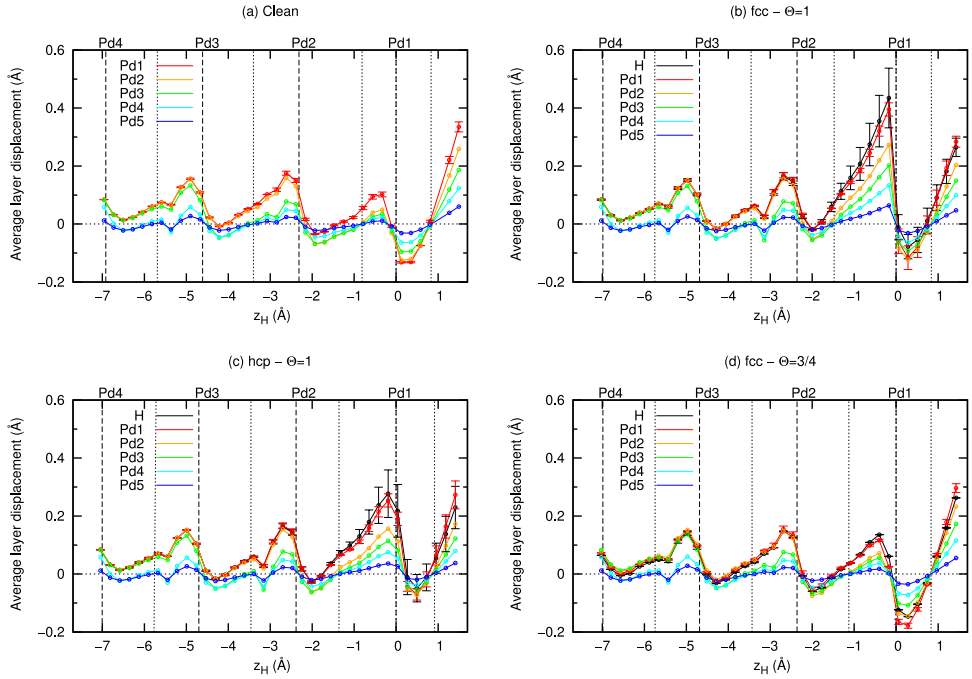

FIG. 3. Average vertical displacements of the surface atomic planes from their equilibrium z coordinate as a function of the impurity z_H coordinate. The vertical dashed lines show the equilibrium heights of the Pd atomic planes, and the dotted lines indicate the equilibrium positions for the H impurity in each host surface. The errorbars indicate the buckling amplitude of the atomic planes, i.e., the height difference between the highest and the lowest lying atom within the plane, for Pd1 and the H coverage layer.

of the clean case than to those of the $\Theta = 1$ cases. Nevertheless, it is important to realize that the largest vertical shifts of the Pd atomic planes of tenths of Å occur when the impurity passes by the diffusion transition states (see Fig. 2), while they are reduced to 0.05-0.07 Å when the H atoms are located at the equilibrium octahedral sites. In-plane relaxations of Pd atoms during penetration of the surface are also small in magnitude. In the clean case, we find a lateral stretch of 0.075 Å at the transition state between S and O_{ss} sites, and 0.020 and 0.038 Å in the $fcc - \Theta = 1$ and $hcp - \Theta = 1$ surfaces, respectively.

Fig. 4 shows the calculated values of the net surface dipole per (2×2) unit cell as the H impurity penetrates the clean and $hcp - \Theta = 1$ surfaces. The μ_0 values extracted directly from Eq. (1) for each z_H value result in a slightly noisy curve due to the small fluctuations in the vacuum potential level caused by the finite thickness of the slab. To avoid this, the data shown in Fig. 4 are smoothed according to this criterion: the vacuum potential at the bottom of the slab is fixed to the value $E_F + \Phi$, where E_F is the Fermi energy of the slab and $\Phi = 5.28$ eV is the calculated clean Pd(111) surface work function. As expected, changes in μ_0 occur when the impurity passes by the near-surface region, but it is soon screened by the metal atoms at heights $z_H < 1$ Å (see Fig. 4), where the μ_0 values of the host surfaces (given in Table I) are retrieved at clean Pd(111). When the impurity is at the S site, it yields $\mu_0 < 0$, as expected for an electron acceptor. On the densely covered surface, conversely, the impurity has the effect of reversing the net negative surface dipole.

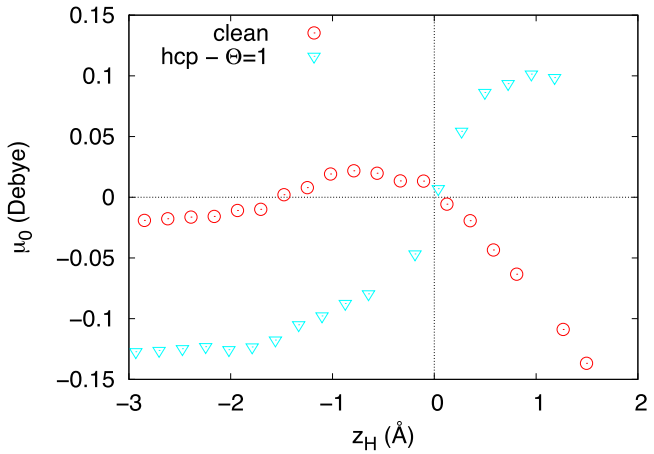

FIG. 4. Surface (spontaneous) dipole for H penetrating the clean and $hcp - \Theta = 1$ covered surfaces. Height $z_H = 0$ corresponds to the relaxed Pd1 height.

B. Effects induced by external electric fields

For each of the four host surfaces, we have calculated the CDD induced by an external static electric field E_{ext} according to Eq. (3). As pointed out in Ref. 37, field emission might happen under application of E_{ext}. The electrons tunnel into the vacuum region if this extends beyond an approximate distance of Φ/E_{ext}. This sets, on the one hand, an upper boundary for the vacuum region size in-between the periodic slabs. On the other hand, the vacuum region must be large enough to allow for a proper description of the charge spilling outside the metal, in other words, to avoid interactions between periodic slab images. In all the settings tested for our supercell calculations, it was not possible to obtain a good compromise between these two conditions neither for $E_{ext} = -0.04$ a.u. nor for fields of larger intensities. For this reason, we restrict ourselves

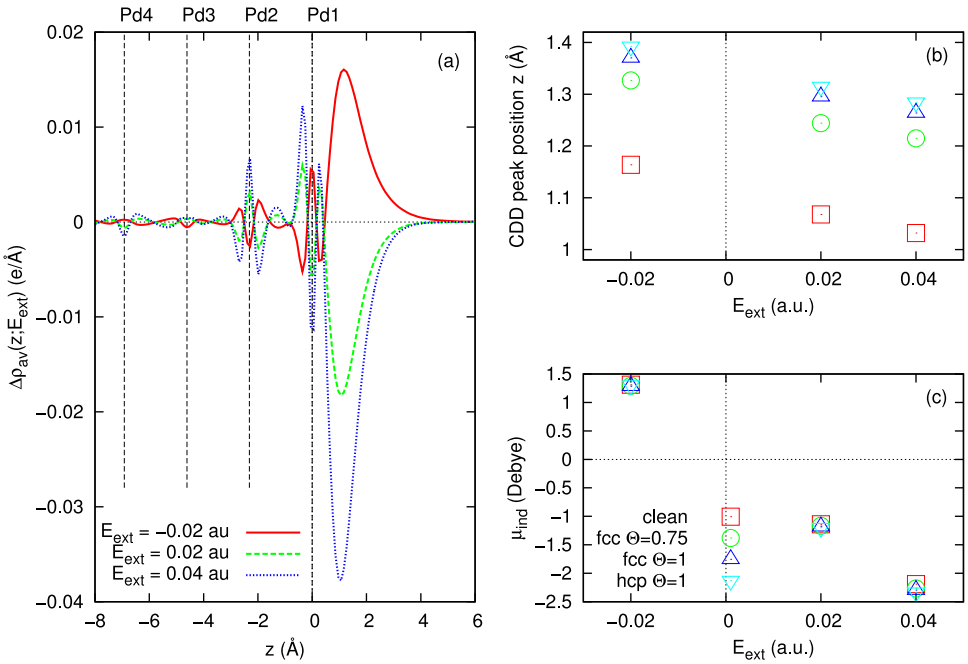

FIG. 5. (a) CDDs for several E_{ext} values in the clean Pd(111) surface as a function of height. The vertical dashed lines indicate the z coordinates of the outer Pd planes of the surface. (b) Positions of the CDD peaks above the surface for several coverages. Height $z = 0$ corresponds to the relaxed Pd1 height in each host surface. (c) Induced dipoles as a function of E_{ext} calculated following Eq. (4).

to reporting the results obtained for $E_{ext} = \pm 0.02, +0.04$ a.u. Fig. 5(a) shows the CDD at the clean surface for these field values as a function of the z coordinate measured from the top Pd layer. The peaks at $z \sim 1$ Å reveal the charge redistribution above the surface (a counteracting redistribution occurs below the bottom layer of the used slab). The figure shows that inside the metal slab, the field is screened out and the CDD shows negligible fluctuations. More charge is displaced when a more intense field is applied, and the positive and negative CDD peaks are consistent with the field direction: charge depletion occurs above and accumulation below the slab for $E_{ext} > 0$. The CDD curves have similar behaviours for different host surfaces, the main difference between the clean and covered slabs being that the CDD peaks lie at a slightly lower z in the former (around 0.15 Å lower). Fig. 5(b) shows the z position of the peaks in the CDD above the slab (see Figure 5(a)) for the studied coverages and E_{ext} values. Fig. 5(c) shows the induced surface dipoles, μ_{ind}, calculated from Eq. (4). They are an order of magnitude larger than the spontaneous μ_0 (see Table I) and only minor differences exist between the clean and H-covered surfaces, since the μ_{ind} values are dominated by the Pd charge density rearrangement.

Once the host surfaces have been characterised, we examine the external electric field effects on the one-dimensional H-Pd interaction potentials of Fig. 2. First of all, we notice that the application of E_{ext} causes negligible changes in the geometries. Thus we can continue to use the atomic coordinates found in the constrained optimisations with $E_{ext} = 0$. The changes in the μ_{ind} values produced by the presence of the impurity (not shown) are also minimal, since, as noted above, they are dominated by the Pd polarizability. The effect of E_{ext} on the potential energies is small, but non-negligible. The energies change <20 meV when the impurity is located below the surface, at $z_H < -1$ Å, and the changes become significant only when the impurity charge is not fully screened by the Pd atoms, as expected, albeit even for $z_H > -1$ Å energy changes are smaller than 80 meV. Fig. 6 shows the variations in the reaction energies and barriers along the impurity penetration pathway of the clean and $hcp - \Theta = 1$ cases.

IV. DISCUSSION

In the aforementioned STM experiments, a lift of the Pd layers is considered as a fingerprint of the existence of subsurface H. For this reason, it is timely to start our discussion with the analysis of the relaxations induced by the impurity under various coverage concentrations. In the experiment by Sykes *et al.*,[1] where hydride patterns are created on a clean Pd(111) surface by manipulation of H diluted in the bulk, the authors report that the heights range of the hydride features varies between 0.1 and 0.6 Å with respect to the clean region of the sample. In our calculations, we observe that, along the diffusion pathway, the Pd layers tend to shift away from a closely lying H impurity (see Fig. 3), moving upward or downward, which reflects a strong Coulomb repulsion effect. Upward shifts are less restrictive, as expected, and therefore they are larger in magnitude.

However, the largest found values do not correspond to local equilibrium positions of the impurity, but to positions close to the transition states along the diffusion pathway. A H atom located at the O_{ss} site induces an upward relaxation of all the upper Pd layers, and the Pd1 z-coordinate, which is the theoretical counterpart of the observed hydride height in STM, is raised by ~0.05 Å (~0.07 Å) in the clean

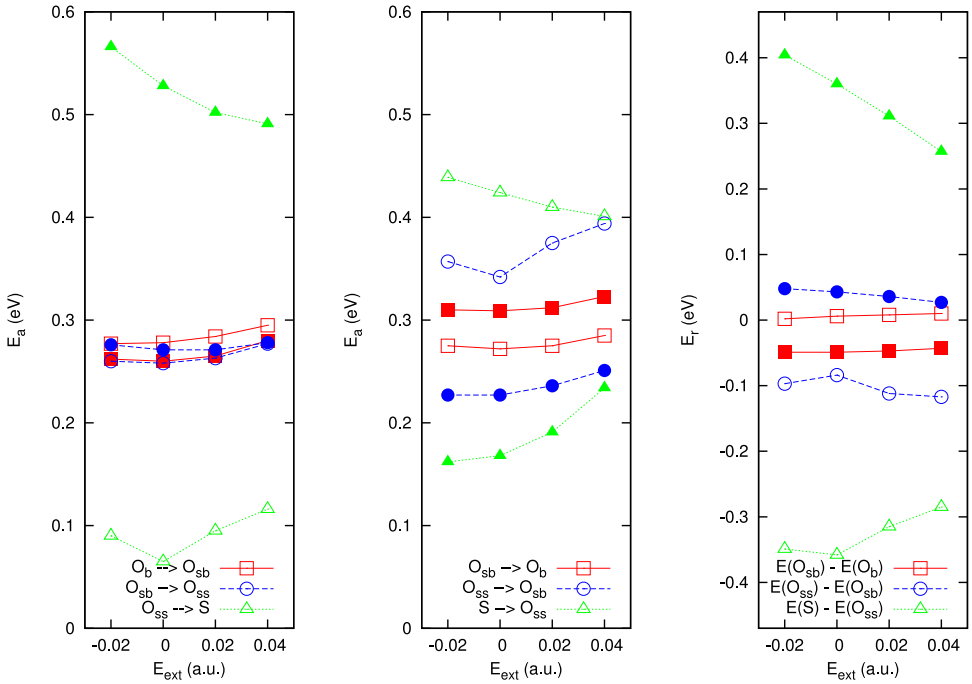

FIG. 6. Diffusion barriers (E_a) and reaction energies (E_r) under the application of E_{ext} for the clean (open symbols) and $hcp-\Theta=1$ covered (filled symbols) surfaces.

(saturated) surface(s). These vertical lattice expansions are in accordance with early quantitative low-energy electron diffraction [LEED-I(V)] studies, which find that the H atoms at octahedral sites induce expansions of the Pd1-Pd2 interplanar distance of 0.05 Å.[9] However, these theoretical results are at apparent variance with the STM experiment. The large lattice expansions of 0.1-0.6 Å are obtained, in our calculations, only when the H impurity lies immediately below a Pd atomic plane close to the transition state for diffusion, and only in the densely covered surfaces (see Fig. 3). Considering that the lattice constant of a hydride of PdH stoichiometry is ~5% larger than that of Pd,[38] one possibility that would yield larger plane expansions is the stacking of H interstitials at O_{ss}- and O_{sb}-like sites. However, it is unlikely that a H-rich surface hydride alone can fully account for protrusions of >0.1 Å. Besides, it is known that both isolated H adatoms on clean Pd and vacancies on 1 ML covered Pd are imaged as large protrusions in topographic STM mode of 0.15 and 0.50 Å, respectively.[39] For this reason, we cannot completely rule out the possibility that the observed heights of the hydride features, of unknown PdH_x composition, are larger than the actual ones. In any case, it is worth noting that, in our calculations, the Pd1 layer in the $\Theta = 1$ covered surfaces lies ~0.08 Å higher than in the clean surface and the adsorption height of the H layer adds an additional ~0.08 Å to the observed height difference with respect to the clean Pd(111). For this reason, we believe that the STM images of the formed hydride nanostructures of Ref. 1 are better explained by a H-covered structure than, as initially proposed in Ref. 1, by a structure with no H on the surface.

We discuss next how the preadsorbed H atoms modify the barriers and reaction energies for H diffusion at the near-surface region. As expected, the presence of H-coverage has a blocking effect on resurfacing processes (see Table II). For instance, the resurfacing barrier raises from 0.065 to 0.189 eV for $\Theta = 0.75$, but even for this rather high coverage the S site is still the most stable. Only at $\Theta = 1$, absorption at the O_{ss} is preferred over adsorption at S site, with resurfacing barriers $E_a(O_{ss} \rightarrow S) > 0.5$ eV. The reverse process, i.e., penetration of the Pd1 layer, requires smaller activation energies: 0.369 and 0.168 eV for adsorbates saturating the *fcc* and *hcp* sites, respectively. The large values of the resurfacing barriers in the saturated surfaces confirm the expected blocking effect for H impurities diffusing from the bulk that attempt to resurface. Nevertheless, this does not guarantee that they will remain at the O_{ss} sites, since the deeper site O_{sb} is slightly more stable and $E_a(O_{ss} \rightarrow O_{sb}) \simeq 0.2$ eV when $\Theta = 1$. Below this coverage, the O_{ss} sites are more stable (by 36-84 meV) than the deeper ones, and the resurfacing barriers are lower than those of transfer to O_{sb} sites.

Based only on the details of the one-dimensional potential energy curves, we can propose the following model for resurfacing of diluted buried H in Pd. The STM current, via an electron-vibration coupling mechanism, triggers diffusion of H atoms inside the sample, which jump from octahedral to tetrahedral cavities and vice versa assisted by quantum tunneling through the barriers, as described in Refs. 16 and 40. The H atoms that eventually reach cavities near a clean region of the surface via these mechanisms will emerge, as shown in Ref. 16, and occupy a *fcc* adsorption site aided by the very low height (65 meV) of the last barrier from a O_{ss} to a S site (see Fig. 2). The latter configuration is much more energetically favourable than the buried sites and the penetration barrier is 0.424 eV, so that at this stage the impurity may either remain at the *fcc* site or diffuse to a neighbouring *hcp* site on the surface surmounting a barrier

of just 0.138 eV located at the bridge site. An alternative resurfacing pathway with similar energy barriers is that from O_{ss} to the surface *hcp* hollow, with $T_{ss,hcp}$ as intermediate site. The barrier for on-surface diffusion is in good agreement with other theoretical works[10] and consistent with the observation of rapid on-surface STM induced diffusion at bias voltages >0.15 V.[19] Note, however, that this diffusion mechanism on the surface will be hampered if many neighbouring surface sites have been occupied by the emerging impurities. If the STM bias application is continued in time, a H-rich coating is formed on the surface, since we have proved that even at a moderate coverage of $\Theta = 0.75$ resurfacing is preferred. The coating causes a blocking effect, and additional impurities that try to reach the surface will be trapped at sites of O_{ss} (and eventually O_{sb}) type, resulting in the Pd atomic plane lifting imaged by STM.[1] At this point, it is important to mention that the electron-vibration coupling diffusion mechanisms do not impose any bias on the directionality of the H jumps (in the theoretical work of Ref. 16 the impurities flow toward the clean surface just because the potential topography itself makes the dynamics prone for resurfacing), which is a fair assumption bearing in mind that the only ingredient in the model able to produce such a bias would be the tip field polarity, and that this has a negligible effect on the potential at $z_H < -1$ Å. We will discuss in detail tip field effects later on, in this section. Since an impurity located at deeper O_{sb} sites can also produce a significant lifting of the outer Pd planes, from the experimental point of view it would seem plausible that the surface remained clean, with empty O_{ss} and filled O_{sb} sites. However, given the calculated potential profile of Fig. 2, it is unlikely that impurities travelling toward the surface under a steady STM charge injection will stop before the $O_{sb} \rightarrow O_{ss}$ barrier if they have been able to overcome the $O_b \rightarrow O_{sb}$ one. We recall that tetrahedral local minima exist along the (staircase-shaped) pathway from the bulk toward the subsurface that make the highest barriers to surmount to be ~0.2 eV. Therefore, the potential topography details point to a densely H-covered surface and added H atoms at O_{ss} or O_{sb} sites as the most likely configuration of the hydride features observed by Sykes *et al.* after manipulation of buried H atoms.

We now turn our attention to other series of STM experiments performed on H-covered Pd(111) where the surface species themselves are also manipulated. On the one hand, at low coverages of <0.33 ML, STM current pulses are able to create small protruding regions that are regarded by Sykes *et al.* as depleted of surface H.[1] Considering the differences in energy barrier heights discussed above (see Table II), it seems clear that the existing surface H atoms will diffuse on the surface rather than penetrate to O_{ss} positions upon application of a STM current pulse. Even at high temperatures, the branching ratio between both processes will be strongly skewed towards on-surface diffusion. If any, penetration may happen under dense coverage conditions with H atoms occupying *hcp* hollows (this implies that both hollow sites must be occupied), where the penetration barrier of 0.168 eV is similar to the barrier for surface diffusion at low coverage, 0.138 eV. However, the experimentally observed protrusion, which is attributed in Ref. 1 to H atoms that have travelled upward from buried regions in the Pd crystal toward O_{ss} sites, must feature *S* occupied sites, too, based on the arguments used above. In the experimental work by Mitsui *et al.*, on the other hand, the manipulation of surface H takes place on a densely covered surface close to 1 ML saturation.[3] Here, injection of STM current results in two types of surface patterning: (i) triangles with $(\sqrt{3} \times \sqrt{3}) - R30°$ periodicity and size of a few tens of nm^2, centred at the tip position, and (ii) small patches of hydrides highly rich in H localised at the boundaries of the triangles, which are imaged as very bright features of sizes <1 nm^2. The reconstructed structure of the former patterned region has coverage $\Theta = 1/3$ or $2/3$, where at least one H atom lies at a *S* site according to former LEED-I(V) studies.[9] These H-depleted triangles are not fully stable, though, and the higher coverage can be gradually recovered over a few minutes at temperatures 40-50 K.[3] Penetration of H below the surface is proposed to be one of the mechanisms contributing to depletion of adsorbates in the vicinity of the tip when the pulses are applied in the dense coverage regime, since the on-surface H diffusion pathway (over the surface bridge sites) must be hindered by many hollow sites being filled with H adsorbates.[3] However, as stated above, penetration is unlikely to happen at non-saturated regions according to our results, which is supported by the fact that there is still some H on the surface at the large triangular patches after pulse application. We have also shown that any buried H will tend to emerge at the non-saturated regions surmounting low barriers of 0.065-0.189 eV, and that the on-surface diffusion barrier is comparable as long as there are empty surface sites. These results are consistent with the observed refilling of the triangles with H.

Summarizing, the results above support the idea that H interstitials diluted in the bulk diffuse upward to end up in subsurface sites only if the surface sites have been previously blocked by other H atoms (otherwise, they will emerge to the surface) and that diffusion on the surface is the preferred route for surface H atoms, while penetration is unlikely. Thus, the experimental evidence of subsurface H must be due to H atoms that were located below the surface before the application of STM pulses. Molecular beams experiments and DFT calculations have shown that the barrier for surface H penetration into Pd subsurface sites is reduced by adsorption of C species[41] and by low Pd coordination (for instance, it is more likely to happen at the edges of Pd nanoparticles).[8] A concerted motion of surface atoms, at high H coverages, can facilitate penetration, too.[42] These processes, despite having low barriers, correspond to narrow regions of the configurations space and require highly dynamical scenarios, achievable under thermal and hyperthermal conditions. In contrast, in the STM experiments under analysis here, the calculations show that penetration events are unlikely (dynamical simulations are currently undergoing with the aim of confirming this trend).

We analyse next our results on the electric field effect on the energetics of H diffusion. Fig. 6 shows the changes in the adsorption wells and diffusion barriers upon application of an external static field, obtained from a DFT calculation where the wavefunctions are self-consistently converged in the presence of the field. Mitsui *et al.* also make use of these type of DFT

calculations to explain their observations.[3] For a wide range of H concentrations at Pd(111), ranging from isolated adsorbates to a surface trilayer of PdH stoichiometry, the authors find that the H adsorption wells are destabilised ∼0.1 eV by external electric fields of intensities ±2 V Å^{-1} (≃0.04 a.u.). The net effect is to drive H atoms away from the high-field regions and, in particular, at intensities ≥3 V Å^{-1} configurations where the *S* and O_{ss} sites are simultaneously occupied are slightly more stable than configurations with occupied *S* sites only. Note that the H binding energies changes reported in Ref. 3 are slightly larger than the ones we find in Fig. 6. Nevertheless, it is important to point out that the quantities of Ref. 3 cannot be directly compared with the data from Fig. 6 (except for the case with one H atom per unit cell) as those literature values represent adsorption energy changes averaged over all the H atoms present in the cell, whereas our calculations show the H-Pd interaction potential changes experienced by a *single* H atom, namely, the diffusing impurity. We observe that the energy changes shown in Fig. 6 are significantly smaller than any of the barriers for penetration or resurfacing, which are listed in Table II in the absence of the field. Also for the mechanism of diffusion on the surface, we find that the bridge site barrier is decreased by only ∼10 meV under the most intense field used in the present work, E_{ext} = 0.04 a.u. Therefore, we extract the important conclusion that the analysis made above on the likelihood and competition of the different H diffusion processes in the outer layers of clean and H-covered Pd(111) remains valid under a typical STM tip induced electric field during a manipulation experiment, of up to around ±2 V Å^{-1}. Much higher field intensities may be realized in STM experiments that will evidently have a more significant impact on the energetics and eventually drive an inversion of the different site stabilities. In fact, this mechanism has already been proposed in the literature to explain NH_3 desorption from Cu(111). This has been theoretically predicted to be a realizable process at negative bias by coupling the molecule dipole to an electric field of ∼1 V Å^{-1}.[43] This intensity corresponds to a threshold situation where the stabilities of the adsorbed state and a desorption-precursor state are inverted, boosting the desorption probability from 0 to 1. In contrast, a IR-laser induced mechanism of vibrational excitation would be much less efficient. In another example, trans-cis reversible isomerization of azobenzene has been experimentally achieved by STM without the interplay of tunneling current at high bias voltages (>2 V).[44] Regrettably, with the methodology used here, we could not find the cell height and dummy charged plane settings that would allow us to safely converge an electron wavefunction for H in Pd with no charge accumulation in the vacuum region for more intense fields.

Finally, it is worth mentioning that the self-consistent convergence of surface charge densities under external electric fields is computationally demanding and very sensitive to some calculation parameters. For that reason, it would be helpful to count on predictions made from calculations performed at E_{ext} = 0. In the Appendix, we show approximations made using values of the surface dipole μ_0 and the polarisability.

Even if a reduced one-dimensional description of the H-surface interaction potential has been considered here, we see that it has a very involved topography. As argued above in the absence of external electric fields, under STM current injection, the H-impurity is expected to behave quasi-thermally at long time scales, governed by the PES minima and barriers. We find that the latter PES features are not greatly changed by fields of up to 2 V Å^{-1}. Therefore, we can reasonably anticipate that the quasi-thermal behaviour will persist in the presence of the tip, at least at the moderate field values discussed in the present work.

V. CONCLUSION

We have performed *ab initio* calculations of H atoms embedded in a Pd(111) surface under various H coverage conditions and external static electric fields. This study is mainly motivated by the STM manipulation experiments of Sykes *et al.* where diluted H interstitials in the bulk region are brought toward the surface and thought to lie at subsurface sites after the STM current pulses have been applied.[1] In the absence of external electric fields, the H-Pd interaction potentials calculated here show that subsurface occupation is weakly stable in the absence of H atoms blocking the resurfacing routes (we find that the barrier for H resurfacing is only 65 meV). Therefore, we conclude that the experimental observation of H occupying subsurface sites after manipulation of diluted H from the bulk must be accompanied by saturation of surface sites with H adsorbates. The inverse process, i.e., penetration of H adsorbates, shows barriers >400 meV, which confirms that during the experiment H is being removed from the bulk and not from the surface. Further support for covered surface configurations is found in the relaxed geometries, which show larger expansions of the Pd atomic planes than the clean surface, in better agreement with experiments. As shown in the work by Mitsui *et al.*,[3] STM manipulation of surface H can be accomplished, too. The results we present here support a model where surface H diffuses *on* the surface and where the observed fingerprints of subsurface H are due to diffusion of atoms that were initially located below the surface.

The external electric fields analysed in the present work (up to 2 V Å^{-1}), which are in the range of typical electric fields exerted by a STM tip, are not intense enough to invert the H-Pd potential energy minima and barrier heights found in the absence of external fields, due to the small surface dipole values and the weak variation of the energy landscape caused by the electric field. In the particular case of surface H manipulation, it had been suggested that diffusion and even penetration of the H atoms could be accomplished by these electrostatic means. Notwithstanding that H transfer by coupling of the surface dipole to a sufficiently high static electric field should not be completely excluded, our results suggest that the efficient H transfer must be dominated by other mechanisms, such as the vibrational excitation by inelastic electron scattering proposed in earlier works.[16,40] The latter mechanism is ruled by the H-Pd potential topography details, but it also depends on the bias voltage and STM current intensity. A detailed dynamical study that considers those ingredients is needed to account for the origin and final

location of the H species more accurately, as well as to get insight into the timescales of the transfer process, which are unavailable in those manipulation experiments.

ACKNOWLEDGMENTS

Financial support by the Gobierno Vasco-UPV/EHU Project No. IT756-13, and the Spanish Ministerio de Economía y Competitividad (Grant No. FIS2013-48286-C02-02-P) is acknowledged. M.B.-R. acknowledges the European Commission (Grant No. FP7-PEOPLE-2010-RG276921) and J.C.T. acknowledges the Deutsche Forschungsgemeinschaft through the Emmy-Noether programme (Project No. TR1109/2-1). Computational resources were provided by the DIPC computing center.

APPENDIX: SURFACE DIPOLE APPROXIMATIONS

In the simplest approximation, the external field contributes a term $-\vec{\mu}_0 \cdot \vec{E}_{ext}$ to the H-Pd potential energy, where the surface dipole μ_0 is given by Fig. 4. Thus, for a typical $E_{ext} = 0.02$ a.u., the largest change in the potential is ∼0.03 eV with the impurity lying at the *S* site. We can also estimate that the contribution of the H dielectric polarizability, using its exact value $\alpha = 9/2a_0^3$ (in atomic units) in isolation, would be ∼0.025 eV, although the CDD curves in Fig. 5(a) indicate that the dominating contributions have their origin in the polarizability of the Pd surface. The model can be improved with lateral interaction of dipoles and substrate induced effects. Since the μ_0 values of the covered surfaces with $\Theta = 1/9, 1/4$ are very similar (see Table I), we can consider that $\Theta = 1/4$ represents a good zero coverage limit, i.e., that the value $\mu_0 = -0.066$ D is the dipole contributed by each H adsorbate. Values for other faces must differ due to a different screening of the adatom charge, which should be more effective the higher the coordination number. The experimentally measured values of $\mu_0 = -0.071$ D for Pd(110)[45] and $\mu_0 = -0.093$ D for Pd(311)[46] confirm this trend. At higher coverages, the increase in Φ is not proportional to the coverage or, in other words, the effective dipole magnitude per adsorbate is smaller than 0.066 D, as dipole-dipole lateral interactions become non-negligible and each individual dipole is depolarised by the electric fields induced by the neighbouring dipoles. Electrostatic models have been proposed in the literature to describe this lateral interaction of dipoles. At a given coverage Θ, if the effect of image dipoles is neglected, the effective dipole per adsorbate in a hexagonal lattice arrangement is[47]

$$\mu_0(\Theta) = \frac{\mu_0(0)}{1 + \alpha F(a)}; \qquad F(a) = 8.89\left(\frac{2}{a^3\sqrt{3}}\right)^{3/2}, \quad \text{(A1)}$$

where a is the distance between adsorbates on the surface and α is their static polarizability. Alternatively, the depolarising effect of dipole images can be considered in the model[48]:

$$\mu_0(\Theta) = \frac{\mu_0(0)}{1 + \alpha(F(a) - 1/4h^3)};$$
$$F(a) = \frac{4\pi}{Ca^3\sqrt{3}}\left[1 + \left(1 + \left(\frac{2h}{Ca}\right)^2\right)^{-3/2}\right], \quad \text{(A2)}$$

where $C = 0.658$ and h is the distance of dipole to the image plane, which we take equal to the H adsorption height. Substituting the values for the *fcc* − Θ = 1 case from Table I, we obtain that the adsorbed H polarizability is $\alpha = 23.37a_0^3$ or $\alpha = 12.64a_0^3$, depending on whether we include image dipoles or not, respectively. Thus, the interaction with the Pd substrate enhances the H polarizability (and thus also the polarizability contribution to the potential energy) by a factor ∼3–5 with respect to the gas phase value. This polarizability term alone already overestimates the typical reaction energies variations as a function of E_{ext} calculated by DFT (see, for example, the $E(S) - E(O_{ss})$ values in Fig. 6(c)), which evidences that, although reasonable estimates can be done, the H-Pd interaction varies non-trivially with the external electric field.

As expressed in Eq. (4), the induced dipole at the host surfaces, μ_{ind}, is the cumulative result of the field-induced rearrangement of the surface charge. Under external fields, μ_{ind} hardly varies with H-coverage due to the overwhelming effect of Pd polarizability (see Fig. 5(c)). In all cases, the charge depletion or accumulation maxima occur well above Pd1, at $z > 1$ Å, and slightly further the larger the H coverage. H-adsorbates displace the CDD peaks by an additional height of 0.20–0.25 Å (see Fig. 5(b)). For each of the host surfaces, the CDD peaks do not occur at the same height at opposite polarities: charge depletion by $E_{ext} > 0$ happens always closer to the surface than charge accumulation by $E_{ext} < 0$. This can be understood in terms of a very simplified picture where dangling (filled) *d*-orbitals, which lie further (closer) to the Pd1 layer, are filled (emptied) under $E_{ext} < 0$ ($E_{ext} > 0$).

[1]E. C. H. Sykes, L. C. Fernandez-Torres, S. U. Nanayakkara, B. A. Mantooth, R. M. Nevin, and P. S. Weiss, Proc. Natl. Acad. Sci. **102**, 17907 (2005).
[2]A. R. Kurland, P. Han, J. C. Thomas, A. N. Giordano, and P. S. Weiss, J. Phys. Chem. Lett. **1**, 2288 (2010).
[3]T. Mitsui, E. Fomin, D. F. Ogletree, M. Salmerón, A. U. Nilekar, and M. Mavrikakis, Angew. Chem., Int. Ed. **46**, 5757 (2007).
[4]A. M. Doyle, S. K. Shaikhutdinov, S. D. Jackson, and H.-J. Freund, Angew. Chem., Int. Ed. **42**, 5240 (2003).
[5]A. M. Doyle, S. K. Shaikhutdinov, and H.-J. Freund, J. Catal. **223**, 444 (2004).
[6]D. Teschner, J. Borsodi, A. Wootsch, Z. Revay, M. Haevecker, A. Knop-Gericke, S. D. Jackson, and R. Schloegl, Science **320**, 86 (2008).
[7]D. Teschner, Z. Revay, J. Borsodi, M. Havecker, A. Knop-Gericke, R. Schloegl, D. Milroy, S. D. Jackson, D. Torres, and Sautet, Angew. Chem., Int. Ed. **47**, 9274 (2008).
[8]W. Ludwig, A. Savara, R. J. Madix, S. Schauermann, and H.-J. Freund, J. Phys. Chem. C **116**, 3539 (2013).
[9]T. E. Felter, E. C. Sowa, and M. A. Van Hove, Phys. Rev. B **40**, 891 (1989).
[10]O. M. Løvvik and R. A. Olsen, Phys. Rev. B **58**, 10890 (1998).
[11]J. F. Paul and P. Sautet, Phys. Rev. B **53**, 8015 (1996).
[12]R. Löber and D. Henning, Phys. Rev. B **55**, 4761 (1997).
[13]N. Ozawa, T. A. Roman, H. Nakanishi, H. Kasai, N. B. Arboleda, Jr., and W. A. Diño, J. Appl. Phys. **101**, 123530 (2007).
[14]P. Ferrin, S. Kandoi, A. U. Nilekar, and M. Mavrikakis, Surf. Sci. **606**, 679 (2012).
[15]J. C. Tremblay and P. Saalfrank, J. Chem. Phys. **131**, 084716 (2009).
[16]J. C. Tremblay, J. Chem. Phys. **138**, 244106 (2013).
[17]J. I. Cerdá, B. Santos, T. Herranz, J. M. Puerta, J. de la Figuera, and K. F. McCarty, J. Phys. Chem. Lett. **3**, 87 (2012).
[18]T. Mitsui, M. K. Rose, E. Fomin, D. F. Ogletree, and M. Salmerón, Surf. Sci. **540**, 5 (2003).
[19]L. C. Fernández-Torres, E. C. H. Sykes, S. U. Nanayakkara, and P. S. Weiss, J. Phys. Chem. B **110**, 7380 (2006).
[20]J. Greeley and M. Mavrikakis, J. Phys. Chem. B **109**, 3460 (2005).
[21]K. Nobuhara, H. Kasai, H. Nakanishi, and A. Okiji, J. Appl. Phys. **92**, 5704 (2002).

[22]J. C. Tremblay and M. Blanco-Rey, "Manipulating interfacial hydrogens at palladium via STM," Phys. Chem. Chem. Phys. (to be published).
[23]P. Giannozzi, S. Baroni, N. Bonini, M. Calandra, R. Car, C. Cavazzoni, D. Ceresoli, G. L. Chiarotti, M. Cococcioni, I. Dabo, A. D. Corso, S. de Gironcoli, S. Fabris, G. Fratesi, R. Gebauer, U. Gerstmann, C. Gougoussis, A. Kokalj, M. Lazzeri, L. Martin-Samos, N. Marzari, F. Mauri, R. Mazzarello, S. Paolini, A. Pasquarello, L. Paulatto, C. Sbraccia, S. Scandolo, G. Sclauzero, A. P. Seitsonen, A. Smogunov, P. Umari, and R. M. Wentzcovitch, J. Phys.: Condens. Matter **21**, 395502 (2009).
[24]D. Vanderbilt, Phys. Rev. B **41**, 7892 (1990).
[25]J. Perdew, K. Burke, and M. Ernzerhof, Phys. Rev. Lett. **77**, 3865 (1996).
[26]H. J. Monkhorst and J. D. Pack, Phys. Rev. B **13**, 5188 (1976).
[27]L. Bengtsson, Phys. Rev. B **59**, 12301 (1999).
[28]B. Meyer and D. Vanderbilt, Phys. Rev. B **63**, 205426 (2001).
[29]T. Roman and A. Gross, Phys. Rev. Lett. **110**, 156804 (2013).
[30]*CRC Handbook of Chemistry and Physics*, 80th ed., edited by D. R. Lide (CRC Press, Boca Raton, 1999).
[31]H. Conrad, G. Ertl, and E. E. Latta, Surf. Sci. **41**, 435 (1974).
[32]W. Dong, V. Ledentu, P. Sautet, A. Eichler, and J. Hafner, Surf. Sci. **411**, 123 (1998).
[33]J. A. Herron, S. Tonelli, and M. Mavrikakis, Surf. Sci. **606**, 1670 (2012).
[34]For the calculation with $\Theta = 1/9$ a supercell of 3×3 lateral periodicity and four layers has been taken, while keeping the same amount of vacuum, where all the atoms except for the bottom Pd layer have been relaxed. For the plane wave basis set, a $5\times5\times1$ special k-point mesh has been used.
[35]G. Henkelman, B. P. Uberuaga, and H. Jónsson, J. Chem. Phys. **113**, 9901 (2000).
[36]G. Henkelman and H. Jónsson, J. Chem. Phys. **113**, 9978 (2000).
[37]P. J. Feibelman, Phys. Rev. B **64**, 125403 (2001).
[38]J. E. Schirber and B. Morosin, Phys. Rev. B **12**, 117 (1975).
[39]T. Mitsui, M. K. Rose, E. Fomin, D. F. Ogletree, and M. Salmerón, Nature **422**, 705 (2003).
[40]M. Blanco-Rey, M. Alducin, J. I. Juaristi, and P. L. de Andres, Phys. Rev. Lett. **108**, 115902 (2012).
[41]K. M. Neyman and S. Schauermann, Angew. Chem., Int. Ed. **49**, 4743 (2010).
[42]A. Gross, ChemPhysChem **11**, 1374 (2010).
[43]P. Saalfrank, J. Chem. Phys. **113**, 3780 (2000).
[44]M. Alemani, M. V. Peters, S. Hecht, K.-H. Rieder, F. Moresco, and L. Grill, J. Am. Chem. Soc. **128**, 14446 (2006).
[45]K. Christmann, Surf. Sci. Rep. **9**, 1 (1988).
[46]D. Farías, P. Schilbe, M. Patting, and K. H. Rieder, J. Chem. Phys. **110**, 559 (1999).
[47]J. Topping, Proc. R. Soc. London A **114**, 67 (1927).
[48]B. L. Maschhoff and J. P. Cowin, J. Chem. Phys. **101**, 8138 (1994).